Mechanical Fault Types Detection in Transformer Windings Using Interpretation of Frequency Responses via Multilayer Perceptron

R. Behkam [1], A. Moradzadeh [2], H. Karami [3], M. S. Naderi [4], B. Mohammadi-Ivatloo [2], G. B. Gharehpetian [1], S. Tenbohlen [5]*

[1]*Department of Electrical Engineering, Amirkabir University of Technology, Tehran, Iran*
[2]*Faculty of Electrical and Computer engineering, University of Tabriz, Tabriz, Iran*
[3]*High-Voltage Research Group, Niroo Research Institute, Tehran, Iran*
[4]*Iran Grid Secure Operation Research Center, Amirkabir University of Technology, Tehran, Iran*
[5]*Institute of Power Transmission and High Voltage Technology, University of Stuttgart, Stuttgart, Germany*

Abstract- *The Frequency Response Analysis (FRA) technique has advantages in identifying faults related to power transformers, but it suffers from the interpretation of frequency responses. This paper presents an approach based on statistical indices and Artificial Neural Network (ANN) methods to interpret frequency responses. The proposed procedure divides frequency responses into four frequency regions based on frequency resonances and anti-resonances. Then, Lin's Concordance Coefficient (LCC) index is used as one of the most appropriate numerical indices to extract features of the four frequency regions. Finally, the Multilayer Perceptron (MLP) neural network is trained by the extracted features to identify and differentiate the types of winding faults. Besides, other intelligent algorithms such as Support Vector Machine (SVM), Extreme Learning Machine (ELM), Probabilistic Neural Network (PNN), and Radial Basis Function (RBF) neural network have been employed to compare the classification results. The proposed techniques have been practically implemented. The Axial Displacement (AD) and Disk Space Variation (DSV) faults are applied as two common mechanical faults in different locations and intensities on the 20kV windings of a 1.6MVA distribution power transformer and their corresponding frequency responses are calculated. Frequency responses calculated from the AD and DSV faults constitute the MLP input data set. The network is trained with part of the input data, and the rest of the data is allocated to validate and test the network. The results show that the suggested method has more proper performance than others using the phase component of the frequency responses in interpreting frequency responses and separation and identifying various mechanical fault types of transformer windings.*

Keyword: *artificial neural network (ANN), frequency response analysis (FRA), mechanical fault, multilayer perceptron (MLP), Power transformer.*

1. INTRODUCTION

Power transformers are regarded as critical components in power systems so that the stability and reliability of the power system depend significantly on their health. This expensive equipment is sometimes seriously damaged due to natural and functional factors. Any damage to the power transformers, in addition to financial and physical damage, endangers the health and stability of the power system [1-3]. Consequently, predicting transformer defects early on is critical for avoiding unforeseen outages and possible blackouts [4,

5]. According to the latest report on the percentage of power transformer defects in Ref. [2], On Load Tap Changer (OLTC) and winding faults account for about 40% and 30% of all transformer faults, respectively. Because of not being easy to access windings compared to tap changers, diagnosis and repair of winding faults are more demanding and more valuable than the OLTC faults [2, 6].

Electrical and mechanical faults are the two major types of transformer winding defects that can be caused by short circuit currents near the transformer terminal, earthquake, improper transport of the transformer, and winding insulation damage [7, 8].

The typical defects that occur in the transformer windings are Radial Deformation (RD), Disk Space Variation (DSV), Axial Displacement (AD), and Short Circuit (SC). The first three faults are called mechanical

faults of the transformer winding, and the occurrence of any of which can lead to the occurrence of the SC fault. Accordingly, early detection of any of these mechanical faults is essential to prevent SCs and severe damages to the transformer windings [2, 6, 9, 10].

So far, the transformer winding fault has been diagnosed by various methods. In the meantime, Frequency Response Analysis (FRA) is one of the best methods for condition monitoring and fault diagnosis of power transformers [11, 12]. The FRA technique is based on comparative analysis; that is, the measurement findings should be compared to certain reference measurements pertaining to the undamaged state of the transformer [13].

The FRA method has been employed as a fault detection technique in transformers in various studies. Most studies have emphasized the standardization measurement process of this method. However, the most crucial challenge that has been observed in most works so far is the interpretation of the results of the frequency responses. In recent years, valuable studies have been conducted to analyze the frequency response measurements results to obtain information about the transformer faults. Main interpretation algorithms can be assorted into three main groups:

- algorithms based on numerical indices and exact calculations [12], [14-17]
- algorithms based on electric circuit models [18-21]
- algorithms based on artificial intelligence (AI) and machine learning techniques [6], [22-26]

The FRA traces are segmented into low-, mid-, and high-frequency bands, and observations are made in each band. In methods based on accurate calculations, the numerical values obtained from the application of statistical indices on the frequency responses of intact and defected conditions at different frequency ranges are compared with the threshold values, and the existence or absence of fault is detected.

In Ref. [12], the frequency responses related to the mechanical faults of windings are interpreted using the calculation of deviations in frequency responses and mathematical comparisons. In another similar work [15], mechanical faults of transformers have been identified via applying the statistical indices on frequency responses and calculating deviations. In Refs. [16] and [17], various threshold values have been provided to determine the fault type using this calculation method. In order to obtain these values and to interpret the FRA results in the offline mode of a

transformer, the need for experienced people and having previous experience about the impact of different faults on any frequency range is one of the weaknesses of this method. In addition, human errors in computational problems and standardization of threshold values for comparing the obtained values are the factors from which that this method suffers.

In Ref. [18], mechanical faults of the winding have been identified by presenting a method based on analyzing circuit model parameters. The proposed method in [18] interprets the frequency responses by comparing the parameters related to the shunt capacitance. The interpretation of frequency responses related to the RD and AD faults to identify their location in Ref. [19] has been performed by a solution based on measurements and evaluation of a physical lumped component transformer circuit. In Ref. [20], the interpretation of frequency responses is performed to identify the type, location, and severity of mechanical faults of the winding based on the analysis of changes in peak and valleys of frequency responses according to the transformer winding circuit model parameters. Performance of methods based on the transformer winding circuit parameters analysis does not depend on the data dimension and the number of available data. However, the main problems of these methods are the need for exact measurements, complex calculations, time-consuming, and inefficiency in issues related to the online monitoring of transformers.

In Ref. [6], two windowing methods and statistical indices have been selected to obtain feature vectors from frequency signatures. Then, the Fisher discriminant analysis (FDA) technique was implemented on the extracted features to reduce their dimensions. Finally, the available features were used as input to the Support Vector Machine (SVM) algorithm to identify and categorize winding faults type and location based on their features. This method must be done in an offline time of the transformer, and it requires high memory and is also time-consuming. In addition, the windowing method is applied without any standard in frequency responses, in which case, there is a high probability of losing the salient features related to the faults in the frequency responses. In Ref. [24], the cross-correlation method has been used to obtain features from the frequency signatures associated with winding faults. Then, considering the extracted features as the input of Artificial Neural Network (ANN) algorithms, fault types and locations have been identified. In Ref. [23], the binary images extracted features from frequency responses related to the RD and

SC defects. The features extracted from the winding faults are then collected as a dataset to be classified and identified via the SVM method. In Refs. [9] and [7], the classification technique based on deep learning called Convolutional Neural Network (CNN) has been utilized to extract features from the frequency responses for detecting the DSV and SC faults, respectively. This method requires a massive dataset to make the exact decision. In Ref. [27], an unsupervised method based on eigenvalues and eigenvectors called principal component analysis is used to extract the features from the frequency responses related to the RD and AD faults. This technique can visually distinguish the faults in a low-dimensional space but does not cover the fault localization. In Ref. [28], ANN using features obtained by statistical indicators was provided to help assess the condition of transformer windings. In this study, all mechanical defects are classified in one class, and the employed ANN could not diagnose different mechanical faults. Besides, only amplitude part of the frequency responses has been considered. In Refs. [29] and [30], heuristic methods have been used to optimize the values of the hyper-parameters in the proposed models. In Ref. [29], the Grasshopper Optimization Algorithm (GOA) was utilized to optimize the value of K in the K-means algorithm using the FRA datasets to detect winding faults. The Particle Swarm Optimization (PSO) method was used in Ref. [30] to reach the optimum number of the clusters in the K-means algorithm using FRA datasets to detect the amount of moisture in the production stage of the transformer. This unsupervised process could be utilized in online motoring systems, but heuristic algorithms in the most realistic environments could be unreliable for all kinds of FRA datasets obtained from different transformers. The K-nearest neighbor (KNN) algorithm was simulated in Ref. [31] to diagnose winding faults. The KNN algorithm is a supervised machine learning algorithm with overfitting problems in classification procedures, especially when the dataset has a complex structure [32]. In Ref. [33], neural networks with a deep learning approach were provided for rotor angle stability assessment. Using the deep learning algorithms requires large data size to be trained; on the other hand, it is time-consuming and needs developed instruments to gather the datasets. In Ref. [34], winding faults effects on the power transformer characterizations. Finite Element Method (FEM) was used to investigate on the electromagnetic forces that change the features of the transformer. An innovative way for reducing losses and optimizing the efficiency of high frequency flyback transformers by rearranging the windings was proposed

in Ref. [35]. It was demonstrated that leakage flux scattering in the core air gap is a significant contributor to the creation of hot-spot points in the windings. As a result, this issue and its potential remedies were examined in further detail.

In this paper, a new method is proposed to improve the previous solutions for interpreting frequency responses and identifying the mechanical faults of the transformer winding. In this paper, feature extraction from frequency responses is implemented using an appropriate numerical index called Lin's Concordance Coefficient (LCC), which is recommended in Ref. [16]. Then, to diagnose the faults, the extracted features are categorized using one of the ANN applications called Multilayer Perceptron (MLP). The AD and DSV faults have been tested and investigated in this paper as two common transformer winding faults. Using the most appropriate index in extracting features and behavioral patterns related to mechanical faults is one of the most important benefits of the work done.

In summary, the paper contributions can be remarked as follows:

- Interpreting the FRA traces via combining appropriate statistical index named LCC and designed intelligent algorithms regarding amplitude and phase components of frequency responses.
- By providing color maps based on appropriate statistical indexes, we can visually depict the variations in frequency responses associated with each fault type, fault location, and fault extent along the windings.
- Examining the influence of various winding faults on each frequency interval, considering the suitable numerical index to gather feature vectors for the intelligent classifiers that have been presented.
- Introducing a new numerical index named fitting percentage (FP) in the application of frequency response interpretation to obtain feature vectors feeding the proposed intelligent classifiers.
- Application of a designed Multi-layer Perceptron (MLP) to interpret the FRA results and compare the classification results with other provided intelligent algorithms such as SVM, ELM, PNN, and RBF. This procedure results in the elimination of non-standard lookup tables created by knowledgeable individuals who interpret the FRA results using precise and sophisticated computations.

The rest of the paper is prepared as follows: Section 2 describes the Sweep Frequency Response Analysis method and the calculation of frequency responses. The

MLP neural network is introduced in Section 3. The experimental setup is presented in Section 4. Section 5 presents the experimental results of fault detection. Finally, the paper is concluded in Section 6.

2. SWEEP FREQUENCY RESPONSE ANALYSIS (SFRA)

Frequency responses related to different states of the transformer winding can be calculated using two methods: Low Voltage Impulse (LVI) and SFRA [2, 13, 36]. Since the results of both methods are the same, in this paper, the desired frequency responses are obtained using the SFRA version. This method states the frequency response in the frequency domain. The SFRA technique uses a pure sinusoidal signal with a constant amplitude and variable frequency as the excitation signal [8]. Frequency sweeping in the desired band will be done by a pure sine wave with fixed amplitude and measuring the output amplitude and its phase shift relative to the input. The computed signals are subsequently sent to the frequency domain through Fast Fourier Transform (FFT). Finally, the frequency response of these signals may be determined by dividing them in the frequency space [8, 13]. In this paper, the frequency response curves have been obtained from 5 kHz up to 1 MHz with the step of 5 kHz.

3. MULTILAYER PERCEPTRON (MLP)

ANNs are powerful tools for regression, estimation, modeling, pattern recognition, and classification in various sciences and industries. The main advantage of these methods is its parallel non-algorithm distributed design for the overall post-learning behavior in general, as well as their capacity to classify novel data patterns [32, 37].

In this paper, The MLP is used as one of the ANN applications to classify the features related to the AD and DSV faults. As Fig. 1 shows, the MLP structure includes an input layer, a hidden layer, and an output layer [38].
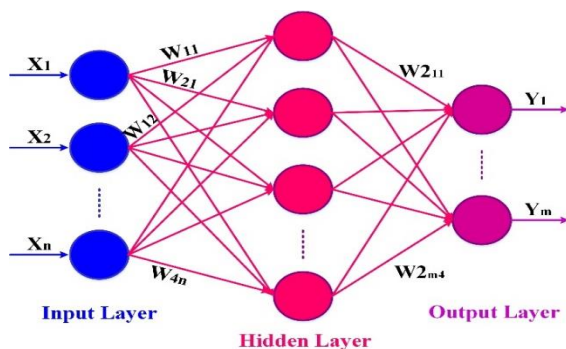

Fig. 1. The structure of MLP

In this structure, the input layer takes the data as the network input and transfers it to the hidden layer. Determining the Bias value and weighting of input data is done in the hidden layer. Finally, the data is categorized based on the assigned values in the output layer, and the output value is estimated [38]. The output vector (Y) in the proposed MLP is calculated from the following equation:

$$Y = f\left(b + \sum_{i=1}^{n} w_i x_i\right) \tag{1}$$

Where x_i is the input vector, w_i represents the weight vector, and b is the bias. The number of neurons in the hidden layer is determined based on the complication of the problem that the MLP wants to solve.

It should be emphasized that in addition to the MLP network, this research compares and evaluates the results using additional techniques such as the SVM, ELM, PNN, and RBF. Details of the ELM method can be found in Ref. [1], a general description of the SVM and RBF methods in Refs. [2-3], and a review of the PNN method details in Ref. [4]. The following findings are obtained by fine-tuning the hyper parameters of the networks mentioned above:

In the structure of the designed PNN and RBF, the sigma value is equal to 0.1. Ten hidden layer neurons are used in the structure of designed MLP in this article. The hyperbolic tangent activation function is utilized in both the hidden layer and the output layer. The Purelin linear activation function is used in the input layer. The Levenberg-Marquardt feed-forward back-propagation algorithm is utilized as a training algorithm. A cubic kernel function is selected for the proposed SVM, and the parameter C is set and tuned as: C=5.

4. EXPERIMENTAL SETUP

This section explains the experimental setup and DSV and AD defects, which were tested on the studied transformer winding. The experimental setup includes a 1-phase winding of a 3-phase transformer. The voltage and power rating of the transformer winding is 20kV/400V and 1600kVA, respectively. The high voltage and low voltage windings comprise 782 turns in 38 discs and 27 turns in two layers, respectively. The parameters related to the specifications of the studied test object are listed in Table 1.

Since the test object is 494 mm high, 5mm displacement is equivalent to about 1.0%. An aluminum cylinder is selected to adjust the potential outer surface of the core. The cylinder is connected to the ground for modeling the capacitive effects between the core and

windings and models the behavior of the core using its outer surface. It should be noted that this aluminum cylinder was used in the measurements related to both the healthy and damaged states of the winding, and its effect was the same in each state. All tests were performed on the HV winding while the LV winding was in the open-circuit state. An impedance analyzer device named the WAYNE KERR 6500B was employed to measure the signals. The basic measurement accuracy is ±0.05%, and the signal source impedance is 50Ω. It should be noted that the measurement of frequency responses in this paper up to 1 MHz was due to the absence of any resonance or anti-resonance for the frequencies higher than 1MHz in the experimental setup used in this paper. Fig. 2-a shows the experimental setup and tested winding. Figs. 2-b and 2-c illustrate the tested DSV and AD defects, respectively.

Table 1. Data of transformer winding used for experiments

Description	Dimension (mm)	Description	Dimension (mm)
Internal radius of LV winding	93	LV winding Conductor	11.8×3.35
External radius of LV winding	106	HV winding Conductor	8.5×2.12
Channel between two layers of LV winding	4	Thickness of insulation paper	0.5
Channel between HV and LV windings	12.5	Height of LV winding	536
Internal radius of HV winding	118.5	Height of HV winding	494
External radius of HV winding	176.5	Radius of core	90

Table 2. Fault Classes

	Fault type	Location	Extent
Defined classes	DSV	Top Double Disk (DD19-16) Middle Double Disk (DD15-12) Bottom Double Disk (DD11-8)	Low (8-12mm) Average(16-20mm) Severe(>20mm)
	AD	N/A	Low (5-20mm) Average(25-40mm) Severe(45-60mm)

Testing the AD fault and investigating its effect was performed by displacing the HV winding height relative to the LV winding in 14 steps. The change in each stage was 5 mm, which generally range of displacement is from 5 mm to 70 mm. Depending on the height of the winding, these changes can be considered from 1% to 14% of the winding height. The DSV fault was performed at the top of the HV winding. For this purpose, ten different locations were considered from the top of the HV winding to apply displacements. The DSV faults were tested at each location with six different intensities (ranging from 6 mm to 40 mm). Hence, 60 different samples (10×6) of DSV faults were analyzed.

As shown in Table 2, there are two fault type classes as DSV and AD. For each fault type, different extents/locations can be defined. Given that this paper aims to identify the type of fault, then all faults related to each type can be considered in the same class. For example, all DSV faults in different winding sections are considered in the same class.
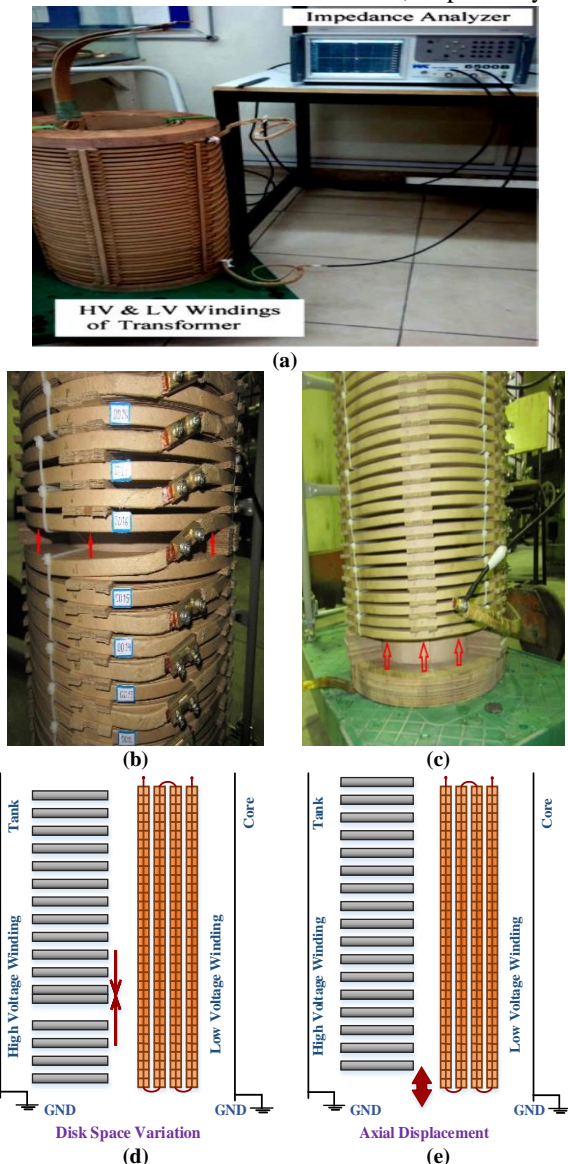

Fig. 2. Experimental setup, (a) winding and impedance analyzer, (b) DSV defect, (c) AD defect (d) schematic view of DSV defect (e) schematic view of the AD defect

5. EXPERIMENTAL RESULTS

FRA method was used to identify the AD and DSV faults in the studied transformer winding. For this purpose, the frequency responses for each of the tested faults were calculated as the following equation:

$$FR = 20\log\left(\left|\frac{V_{in}(f)}{I_{out}(f)}\right|\right) \qquad (2)$$

Where, FR shows the frequency response, $V_{in}(f)$ is the input voltage, and $I_{out}(f)$ represents earth current.
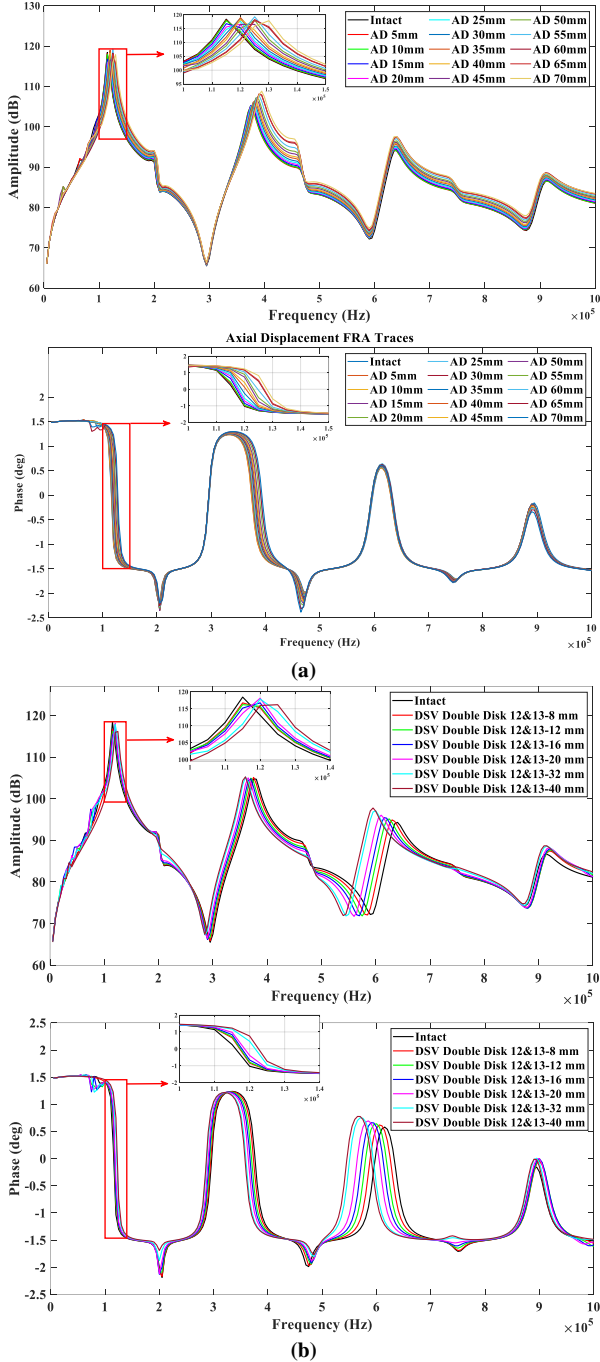
Axial Displacement FRA Traces

(a)

(b)

Fig. 3 Bode diagrams of frequency responses related to the tested mechanical faults in the winding:
(a) AD, (b) DSV

It should be noted that according to the comparative approach of the FRA method, the frequency response related to the healthy state was calculated to be compared with the damaged states before applying the fault on the winding. Fig. 3 illustrates the frequency responses in the healthy and damaged states, including AD and DSV, with different intensities.

Evaluating the frequency responses and observing the changes in the frequency range and their phase indicates the physical defects in the winding. However,

interpretation of frequency responses to identify each fault's exact type and location is challenging and requires complex calculations. The LCC index extracts the features from the amplitude and phase parts of the frequency response curves to solve the mentioned problem in this paper. Then, the extracted features are categorized by the MLP neural network to identify the type of each fault in the winding. Fig. 4 shows the suggested fault diagnosis technique flowchart in this paper.
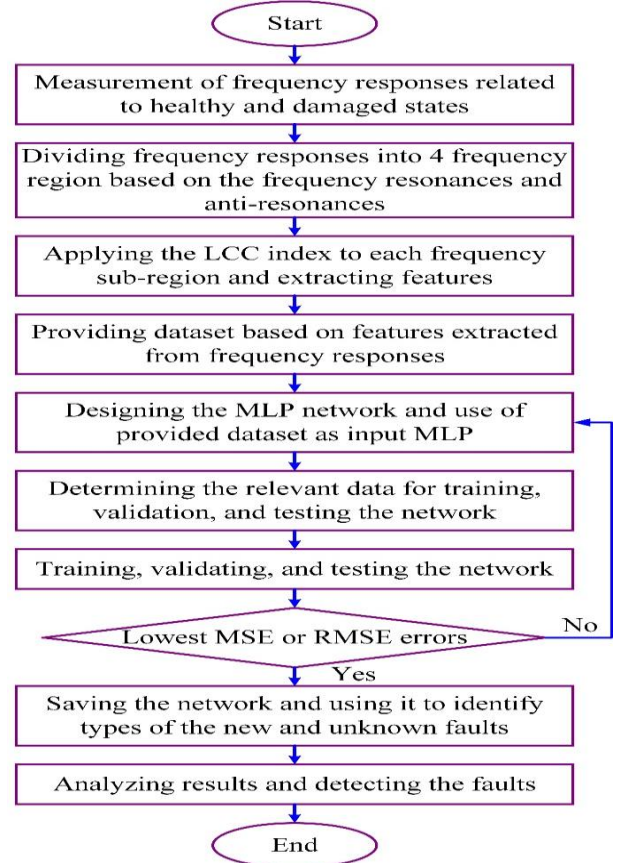

Fig. 4. Flowchart of the fault diagnosis method in this paper

The LCC index is applied to the frequency responses based on the following equation:

$$LCC = \frac{2S_{XY}}{\left(\bar{Y} - \bar{X}\right)^2 + S_Y^2 + S_X^2} \tag{3}$$

$$S_{XY} = \frac{1}{N}\sum_{i=1}^{N}\left(X(i) - \bar{X}\right)\left(Y(i) - \bar{Y}\right) \tag{4}$$

$$S_Y^2 = \frac{1}{N}\sum_{i=1}^{N}\left(Y(i) - \bar{Y}\right)^2 \tag{5}$$

$$S_X^2 = \frac{1}{N}\sum_{i=1}^{N}\left(X(i) - \bar{X}\right)^2 \tag{6}$$

$$\bar{Y} = \frac{1}{N}\sum_{i=1}^{N}Y(i) \tag{7}$$

$$\bar{X} = \frac{1}{N}\sum_{i=1}^{N}X(i) \tag{8}$$

Where X is the amplitude or phase vectors of the intact frequency responses, Y represents the amplitude or phase vectors of the defected frequency responses. $X(i)$ and $Y(i)$ demonstrate the *i-th* elements of these vectors, and N represents the total number of samples in the selected frequency region.

After calculating the frequency responses and determining the classes associated with each error, the next step is to extract the features and collect the input dataset. Table 3 lists the extracted features from the various components of the frequency responses, where $F_c^k(i)$ shows the computed index at the i-th frequency range for the c-th case of k-th fault type. The measurement is performed in the range of 5 kHz up to 1MHz with the steps of 5 kHz. The number of points at each measurement (n) equals 200. k shows the class number, and c denotes the case number corresponding to that class.
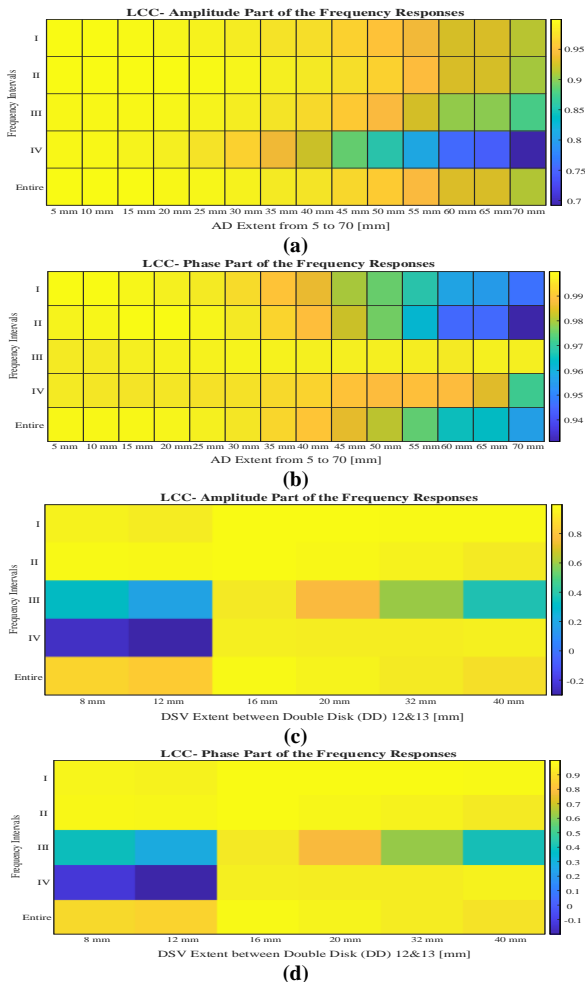

Fig. 5. Visualization of extracted features based on statistical index by color maps representing (a) AD extent from 5 to 60 mm considering amplitude component of frequency responses (b) AD extent from 5 to 60 mm considering phase component of frequency responses (c) DSV extent between Double Disk (DD) 12&13 considering amplitude component of frequency responses (d) DSV extent between Double Disk (DD) 12&13 considering phase component of frequency responses

In the data obtained from the measurements related to the experimental case study, there are four resonance and anti-resonance points at equal distances from each other. The distances between these points are considered as the frequency domain for obtaining the feature vector by the LCC statistical index. From the presented curves, it can be seen that the most displacement of the curves is between successive points of resonance and anti-resonance, so the features obtained in these intervals can show the changes of the signatures appropriately. Given that the frequency of resonances and anti-resonances, the frequency intervals are (5-225 kHz), (225-500 kHz), (500-775 kHz), and (775-1000 kHz).

To facilitate visualization of all the extracted characteristics from FRA traces, the index values between the amplitude and phase components of the healthy and defected frequency responses (DSV and AD) along with the winding are depicted in Fig. 5 as color maps. The horizontal axes illustrate the severity of the DSV fault between DD12&13, as well as the AD fault along with the winding. The vertical axis depicts the frequency regions in each case. As the LCC index approaches one in a given frequency interval, corresponding traces correlate more with intact and defect states. When the index is close to zero, the traces of the healthy and defected conditions are less similar, indicating low correlation. The brighter areas associated with the LCC index demonstrate that the defected traces have a higher correlation with the intact trace. The following describes the figures used in this case study to illustrate the statistical index.

LCC: Given that the higher values of this index indicate a stronger link between the defected and intact condition traces, the third and fourth frequency intervals are considerably influenced by the DSV fault. The AD fault has a significant effect on the fourth frequency region.

Using intelligent classifiers makes it possible to identify winding defects based on the different patterns available. Therefore, the statistical index can aid the intelligent classifier in diagnosing the fault types that occurred in the transformer windings; besides, the statistical index can also be used to detect the severity and location of the faults based on the color map patterns. In future studies, this issue can be addressed. The features extracted from the frequency responses by the LCC index constitute the MLP input dataset. It should be noted that the number of faults tested in the winding is 74 samples. Each frequency response to extract the feature is divided into four frequency sub-

bands. A matrix in dimensions of 74×4 is available as input data. Each row of this matrix corresponds to a mechanical fault, and the number of columns represents the extracted features associated with each fault sample.

The MLP acts like a decision-making unit to identify the fault type in the winding. As mentioned, the target of MLP is the type of defection regardless of its severity and location. The training dataset is used to adjust the weight of connections between neurons and bias to estimate the relationship between input and output variables. After estimating the prediction model and forming a trained network, validation data is used to validate the network. Finally, the test dataset tests and evaluates the trained or saved network. The designed MLP and other intelligent classifiers are trained using 70% of the data. Each network validation and the test steps use 15% of the data. To precisely compare the performance of the designed intelligent networks, the accuracy metric, proportion of the number of true predictions to the number of all predictions, has been calculated and listed for training, validation, and test datasets in Table 4. The Mean values of the accuracies for all datasets considering the amplitude and phase parts have been provided, which show that the phase part of the frequency responses can produce more appropriate features feeding the intelligent classifiers to distinguish mechanical defects of the windings.

Table 3. Features for fault type classification

Classes & Cases	Index #1		
	Frequency region		
	$i = 1$	…	n
DSV k =1 $C_1 = 60$	$F_1^1(1)$ ⋮ $F_{C_1}^1(1)$	…	$F_1^1(n)$ ⋮ $F_{C_1}^1(n)$
AD k =2 $C_2 = 14$	$F_1^2(1)$ ⋮ $F_{C_2}^2(1)$	…	$F_1^2(n)$ ⋮ $F_{C_2}^2(n)$

Table 4. Accuracy values of proposed intelligent classifiers considering amplitude and phase components of frequency responses and different parts of dataset

Index	Net.	Part of FR	Acc. for Train data	Acc. for Val. data	Acc. for test data	Acc. for all data
LCC	MLP	Amp.	88.5 %	81.8 %	72.7 %	85.1 %
		Phase	94.2 %	100 %	90.9 %	94.6 %
	SVM	Amp.	84.6 %	72.7 %	63.6 %	79.7 %
		Phase	90.4 %	90.9 %	81.8 %	89.2 %
	ELM	Amp.	80.8 %	63.6 %	63.6 %	75.7 %
		Phase	86.5 %	81.8 %	72.7 %	83.8 %
	PNN	Amp.	76.9 %	54.5 %	45.5 %	68.9 %
		Phase	78.8 %	63.6 %	54.5 %	73 %
	RBF	Amp.	63.5 %	45.5 %	45.5 %	58.1 %
		Phase	75 %	54.5 %	45.5 %	67.6 %
Mean value of accuracies for all dataset considering phase part						73.5 %
Mean value of accuracies for all dataset considering amplitude part						81.6 %
Net. : Network or Intelligent classifier, FR: Frequency Response, Acc.: Accuracy, Val.: Validation, Amp. : Amplitude						

Fig. 6 demonstrates that the designed MLP utilizing the feature vectors obtained from the phase part of the frequency response traces outperforms the other intelligent algorithms in diagnosing mechanical winding faults. The accuracy evaluation metric for the test dataset is the highest value (90.9 %) for the MLP considering the phase component. In the following, more detailed evaluations about the performance of the proposed MLP using the phase component of the frequency responses have been provided. Fig. 7 shows the prediction results of the MLP network considering the phase component of the frequency responses for training, validation, and test data. The results in this figure are evaluated using the accuracy coefficient (R) evaluation index. The R-index is defined as follows:

$$R = \frac{\sum_{i=1}^{N}\left(X_i - \bar{X}\right)\left(Y_i - \bar{Y}\right)}{\sqrt{\sum_{i=1}^{N}\left(X_i - \bar{X}\right)^2 \sum_{i=1}^{N}\left(Y_i - \bar{Y}\right)^2}} \qquad (9)$$

Where X_i, $\bar{X}$, Y_i, and $\bar{Y}$ represent the target value, average of target values, output value, and average of output values, respectively.
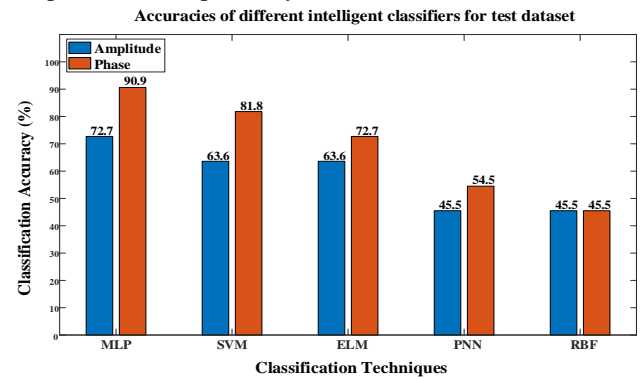

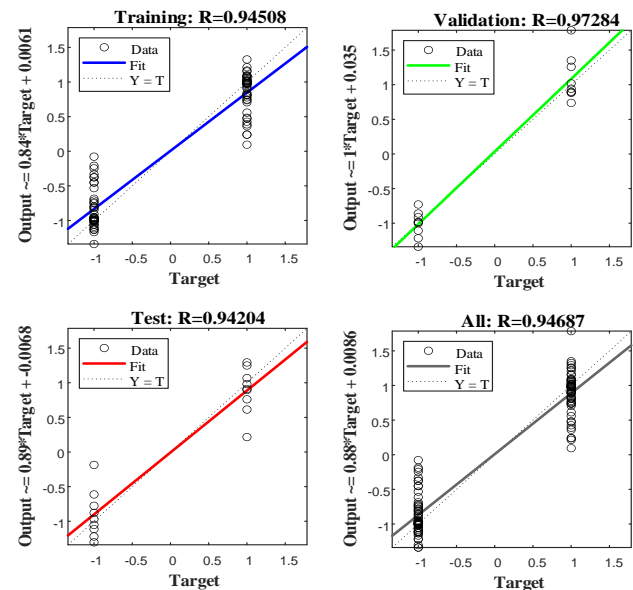**Fig. 6. Accuracy values of intelligent classifiers considering test dataset**

Fig. 7. Results related to the training, validation, and test of the MLP network
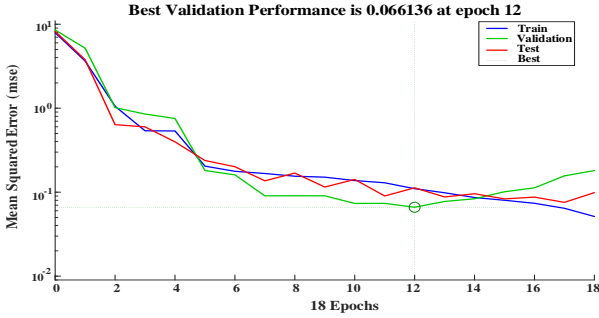
Fig. 8. Error-values for training, validation, and test of the MLP network in the form of MSE
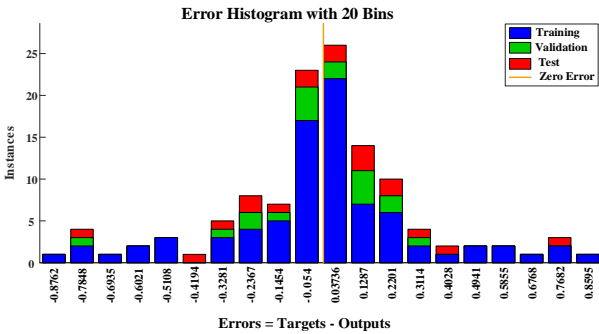

Fig. 9. Error values for testing the MLP network in the form of a histogram

It can be seen that the network is able to detect the types of AD and DSV faults in the training, validation, and test steps with the R values of 0.94508, 0.97284, and 0.94204, respectively. The values obtained in this state show the appropriate correlation between the input data and the predicted values for each target. Calculating and assessing the errors corresponding to the network performance is one of the most important issues to consider when using the ANNs. Fig. 8 shows the training, validation, and testing performance of the MLP network in the form of Mean Squared Error (MSE). The MSE is one of the performance evaluation indicators that is obtained by Eq. (10).

$$MSE = \frac{1}{N}\sum_{i=1}^{N}\left(X_i - Y_i\right)^2 \qquad (10)$$

Another important evaluation factor in ANN applications is determining the range of test errors in predicting new data. In this case, the maximum prediction error of new and unknown data is determined in the test stage. Fig. 9 depicts the test error of the trained MLP network in the form of a histogram. As the results show in Fig. 9, the maximum error values for network testing are close to zero. This result emphasizes the proper performance of the network in testing and identifying types of AD and DSV faults.

The presented results show the ability of the LCC index to extract features from frequency responses related to AD and DSV faults and the proper performance of the MLP in distinguishing and

identifying the type of each fault based on the phase component of the frequency responses. It should be noted that the input dataset has a great impact on network performance, and the prediction results by ANN are highly dependent on it. Therefore, proper network performance also confirms the accuracy and capability of the LCC index. The designed network can now detect new types of AD and DSV defects. In addition, it should be noted that the proposed method can be applied for identifying all faults related to the transformers used in the power system as future work.

6. CONCLUSIONS

Fault diagnosis in power transformers by the FRA method has caused many challenges due to problems related to the interpretation of frequency responses. In this paper, a new approach based on numerical indices and the use of ANN is proposed to interpret frequency responses and identify the type of winding mechanical faults. The LCC was utilized as an approved numerical index to extract the feature from frequency responses, and the designed MLP method was used to detect the type of faults. In order to implement the proposed method, the AD and DSV faults were tested as two common mechanical faults in the 20kV winding of a 1.6MVA distribution power transformer. Frequency responses related to the healthy state and all faults tested in the winding were calculated. The LCC index considering amplitude and phase components of the frequency responses extracted features from all four regions by dividing the frequency responses into four frequency intervals based on resonances and anti-resonances frequency. In order to compare the classification results, other intelligent algorithms such as SVM, ELM, PNN, and RBF were provided. The extracted features were used as intelligent classifier inputs. The results show the ability and appropriate performance of the MLP using the phase component of the frequency responses in distinguishing and identifying the types of AD and DSV faults. It must be mentioned that the proposed procedure can be applied for any transformer. The training data must first be obtained using a sample transformer with similar specifications, which is a costly approach, or from the simulation results of the transformer, similar to many previous studies. This means that for each type of transformer, a simulated model must be developed and verified by the measurement results. Then, different types of faults can be applied to this model in order to generate training data. Consequently, the saved network can be employed to identify type of new faults based on the pattern of each fault.

REFERENCES

[1] O. Arguence and F. Cadoux, "Sizing power transformers in power systems planning using thermal rating", *Int. J. Electr. Power Energy Syst.*, vol. 118, pp. 105781, 2020.

[2] A. Moradzadeh et al., "Locating inter-turn faults in transformer windings using isometric feature mapping of frequency response traces", *IEEE Trans. Ind. Inf.*, 2020.

[3] A. Ardeshiri et al., "Introduction and literature review of power system challenges and issues" in Application of machine learning and deep learning methods to power system problems, *Springer*, 2021.

[4] Z. Babaei and M. Moradi "Novel method for discrimination of transformers faults from magnetizing inrush currents using wavelet transform", *Iranian J. Sci. Tech. Trans. Electr. Eng.*, 2021.

[5] R. Behkam et al., "Generalized regression neural network application for fault type detection in distribution transformer windings considering statistical indices", *Int. J. Comput. Math. Electr. Electron. Eng.*, Vol. 41, pp. 381-409, 2022.

[6] H. Tarimoradi and G. B. Gharehpetian, "Novel calculation method of indices to improve classification of transformer winding fault type, location, and extent", *IEEE Trans. Ind. Inf.*, vol. 13, no. 4, pp. 1531-40, 2017.

[7] A. Moradzadeh and K. Pourhossein, "Short circuit location in transformer winding using deep learning of its frequency responses", *Proc. 2019 Int. Aegean Conf. Electr. Machines Power Electron.,*, 2019.

[8] Y. Akhmetov et al., "A new diagnostic technique for reliable decision-making on transformer FRA data in inter-turn short-circuit condition", *IEEE Trans. Ind. Inf.*, 2020.

[9] A. Moradzadeh and K. Pourhossein, "Location of disk space variations in transformer winding using convolutional neural networks", *54th Int. Universities Power Eng. Conf.*, 2019.

[10] E. Rahimpour et al., "Transfer function method to diagnose axial displacement and radial deformation of transformer windings", *IEEE Trans. Power Del.*, vol. 18, no. 2, pp. 493-505, 2003.

[11] K. Pourhossein et al., "A probabilistic feature to determine type and extent of winding mechanical defects in power transformers", *Electr. Power Syst. Res.*, vol. 82, no. 1, pp. 1-10, 2012.

[12] E. Rahimpour, M. Jabbari, and S. Tenbohlen, "Mathematical comparison methods to assess transfer functions of transformers to detect different types of mechanical faults", *IEEE Trans. Power Del.*, vol. 25, no. 4, pp. 2544-55, 2010.

[13] R. Khalili Senobari, J. Sadeh, and H. Borsi, "Frequency response analysis (FRA) of transformers as a tool for fault detection and location: A review", *Electr. Power Syst. Res.*, vol. 155. pp. 172-83, 2018.

[14] M. H. Samimi and S. Tenbohlen, "FRA interpretation using numerical indices: State-of-the-art", *Int. J. Electr. Power Energy Syst.*, vol. 89, pp. 115-25, 2017.

[15] M. H. Samimi et al., "Evaluation of numerical indices for the assessment of transformer frequency response", *IET Gener. Trans. Distrib.*, vol. 11, no. 1, pp. 218-27, 2017.

[16] M. Tahir, S. Tenbohlen, and S. Miyazaki, "Analysis of statistical methods for assessment of power transformer frequency response measurements", *IEEE Trans. Power Del.*, 2020.

[17] M. Bigdeli, D. Azizian, and G. B. Gharehpetian, "Detection of probability of occurrence, type and severity of faults in transformer using frequency response analysis based numerical indices", *Measurement*, vol. 168, pp. 108322, 2021.

[18] S. Maulik and L. Satish, "Localization and estimation of severity of a discrete and localized mechanical damage in transformer windings: Analytical approach", *IEEE Trans. Dielectrics Electr. Insulation*, vol. 23, pp. 1266-74, 2016.

[19] D. Pham and E. Gockenbach, "Analysis of physical transformer circuits for frequency response interpretation and mechanical failure diagnosis", *IEEE Trans. Dielectrics Electr. Insulation*, vol. 23, pp. 1491-9, 2016.

[20] K. Ragavan and L. Satish, "Localization of changes in a model winding based on terminal measurements: experimental study", *IEEE Trans. Power Del.*, vol. 22, no. 3, pp. 1557-65, 2007.

[21] A. Torkaman, V. Naeini, "Recognition and location of power transformer turn to turn fault by analysis of winding imposed forces", *J. Oper. Autom. Power Eng.*, vol. 7, pp. 227-34, 2019.

[22] S. Bagheri, Z. Moravej, and G. B. Gharehpetian, "Classification and discrimination among winding mechanical defects, internal and external electrical faults, and inrush current of transformer", *IEEE Trans. Ind. Informatics*, vol. 14, no. 2, pp. 484-93, 2018.

[23] Z. Zhao et al., "Diagnosing transformer winding deformation faults based on the analysis of binary image obtained from FRA signature", *IEEE Access*, vol. 7, pp. 40463-74, 2019.

[24] A. J. Ghanizadeh and G. B. Gharehpetian, "ANN and cross-correlation based features for discrimination between electrical and mechanical defects and their localization in transformer winding", *IEEE Trans. Dielectrics Electr. Insulation*, vol. 21, pp. 2374-82, 2014.

[25] A. Moradzadeh and K. Pourhossein, "Early detection of turn-to-turn faults in power transformer winding: an experimental study", *Proc. 2019 Int. Aegean Conf. Electr. Machines Power Electron.*, 2019.

[26] Z. Zhao et al., "Interpretation of transformer winding deformation fault by the spectral clustering of FRA signature", *Int. J. Electr. Power Energy Syst.*, vol. 130, 2021.

[27] K. Pourhossein et al., "A vector-based approach to discriminate radial deformation and axial displacement of transformer winding and determine defect extent", *Electr. Power Components Syst.*, vol. 40, pp. 597-612, 2012.

[28] T. Mehran and S. Tenbohlen. "Transformer winding condition assessment using feedforward artificial neural network and frequency response measurements", *Energies*, vol. 14, no. 11, 2021.

[29] M. Bigdeli and A. Abu-Siada, "Clustering of transformer condition using frequency response analysis based on k-means and GOA", *Electr. Power Syst. Res.*, vol. 202, 2022.

[30] M. Bigdeli, "Hybrid k-means-PSO technique for transformer insulation moisture determination in the production stage based on frequency response analysis", *Iran. J. Electr. Electron. Eng.*, vol. 18, 2022.

[31] M. Bigdeli, "Performance of mathematical indices in

transformer condition monitoring using k-NN based frequency response analysis", *AUT J. Electr. Eng.*, vol. 53, no. 1, 2021.

[32] S. Haykin, Neural Networks and Learning Machines, vol. 3. 2008.

[33] M. Shahriyari and H. Khoshkhoo, "A deep learning-based approach for comprehensive rotor angle stability assessment", *J. Oper. Autom. Power Eng.*, vol. 10, no. 2, 2022.

[34] V. Behjat, A. Shams, V. Tamjidi, "Characterization of power transformer electromagnetic forces affected by winding faults", *J. Oper. Autom. Power Eng.*, vol. 6, no. 1, 2018.

[35] A. Zakipour et al., "Efficiency improvement of the flyback converter based on high frequency transformer winding rearrangement", *J. Oper. Autom. Power Eng.*, vol. 8, no. 3, 2020.

[36] J. Secue, E. Mombello and C. Cardoso, "Review of sweep frequency response analysis -sfra for assessment winding displacements and deformation in power transformers", *IEEE Latin America Trans.*, vol. 5, no. 5, pp. 321-8, 2007.

[37] A. Moradzadeh and K. Pourhossein, "Early detection of turn-to-turn faults in power transformer winding: an experimental study", P*roc. 2019 Int. Aegean Conf. Electr. Machines Power Electron.*, 2019.

[38] A. Moradzadeh et al., "Performance evaluation of two machine learning techniques in heating and cooling loads forecasting of residential buildings", *Appl. Sci.*, vol. 10, no. 11, p. 3829, 2020.

[39] G. Bin Huang, Q. Y. Zhu, and C. K. Siew, "Extreme learning machine: A new learning scheme of feedforward neural networks", *IEEE Int. Conf. Neural Net. Conf. Proc.*, 2004.

[40] V. Jakkula, "Tutorial on Support Vector Machine (SVM)", *Sch. EECS, Washingt. State Univ.*, 2011.

[41] R. Segal, M. Kothari, and S. Madnani, "Radial basis function (RBF) network adaptive power system stabilizer", *IEEE Trans. Power Syst.*, vol. 15, no. 2, pp. 722-7, 2000.

[42] H. Lin, T. Liang and S. Chen, "Estimation of battery state of health using probabilistic neural network", *IEEE Trans. Ind. Informatics*, vol. 9, no. 2, pp. 679-85, 2013.